

DOI: 10.1002/anie.200502632

Ru Nanoparticles Immobilized on Montmorillonite by Ionic Liquids: A Highly Efficient Heterogeneous Catalyst for the Hydrogenation of Benzene**

Shiding Miao, Zhimin Liu,* Buxing Han, Jun Huang, Zhenyu Sun, Jianling Zhang, and Tao Jiang

The design of nanocomposites consisting of functional metals and different matrices is a promising research area for the fabrication of a variety of catalysts, adsorbents, and optical and electrical devices. Montmorillonite (MMT), which is a type of naturally occurring clay, can be structurally defined as layers of negatively charged two-dimensional silicate sheets that are separated by interlayer cationic species with a high exchange ability for other cations.^[1] Such layered materials have been used as host materials for the preparation of composites and have potential applications in catalysis, separation, and the optical and electrical fields.^[2] For example, Pd nanoparticles deposited on MMT with surfactants exhibit a high selectivity for the partial hydrogenation of 1-phenyl-1-pentyne to 1-phenyl-*cis*-1-pentene,^[3] and Sc³⁺-exchanged MMT has been demonstrated to function as an efficient catalyst for the Michael reaction.^[4] For MMT-based catalysts, the catalytic nanoparticles are generally intercalated into the interlayer spaces or deposited on the outer surfaces of MMT with the aid of surfactants or polymers.^[5,6]

In recent years, room-temperature ionic liquids (ILs) have attracted much attention due to their unusual properties, especially their extremely low vapor pressure, high thermal and good chemical stability, and excellent solvent power for organic and inorganic compounds, and they have been widely utilized as environmentally benign solvents for different processes, including chemical reactions^[6] and separations.^[7] ILs are also attractive media to stabilize metal nanoparticles.^[8] Recently, Pd nanoparticles immobilized on the molecular sieve SBA-15 by 1,1,3,3-tetramethylguanidinium lactate have been found to exhibit high catalytic activity for hydrogenation reactions.^[9]

Ruthenium catalysts are important catalysts for the hydrogenation of aromatic compounds, and have been extensively investigated.^[10] However, the development of a

simpler and more efficient method for the preparation of Ru catalysts is still a challenge in nanocatalysis. As mentioned above, MMT possesses negatively charged, two-dimensional silicate sheets with cationic species, and ILs are composed entirely of ions. The combination of MMT and ILs may therefore provide a new way to prepare highly efficient catalysts. Herein, we report the immobilization of Ru nanoparticles onto MMT using the IL 1,1,3,3-tetramethylguanidinium trifluoroacetate ([TMG][TFA]) and their application in the catalytic hydrogenation of benzene. To the best of our knowledge, this is the first synthesis of a nanocatalyst that involves loading catalytic metal nanoparticles onto MMT with an IL.

The IL used was synthesized by following previously reported procedures.^[11] To synthesize the catalyst, Na-MMT was first treated three times with an aqueous solution of [TMG][TFA] to exchange the Na cations with those of the IL (TMG-MMT). After filtration and washing three times with distilled water, TMG-MMT was dispersed in an aqueous solution of RuCl₃ with stirring in order to adsorb Ru³⁺ and form TMG-MMT/RuCl₃ composites. The solvent was then removed from the solution by evaporation and the Ru/MMT catalyst (catalyst A) was obtained after hydrogenation at 220 °C for 2 h.

The as-prepared catalyst A was used for the hydrogenation of benzene. The results are listed in Table 1. It is clear that catalyst A is very active for the hydrogenation of benzene to cyclohexane, with a catalytic activity that is comparable or superior to Ru-cluster-based catalysts. For comparison, the TOFs of [(η⁶-C₆H₆)(η⁶-C₆Me₆)₂Ru₃(μ₃-O)(μ₂-H)₃][BF₄] at 110 °C^[12] and [(η⁶-C₆H₆)₄Ru₄(μ₃-H)₄]Cl₂ at 90 °C and a hydrogen pressure of 6.0 MPa^[13] in ionic liquids are 3644 and 364 mol benzene per mol Ru per hour, respectively.

Our Ru/MMT nanocatalyst is a heterogeneous catalyst, which means that it is superior to homogeneous catalysts in that it can be easily separated from the products and can be used in a fixed-bed process. Catalyst A was reused for a further four runs under the same reaction conditions without any significant loss of activity (entries 6–9). This confirms that it is very stable. We also performed benzene hydrogenation with the traditional Ru/C and Ru/Al₂O₃ catalysts under the same conditions; these results are also given in Table 1 (entries 15–18). Comparing entries 2 and 17, it can be seen that our Ru/MMT catalyst has a much higher activity than Ru/Al₂O₃. The Ru/MMT catalyst is also more active than Ru/C (see entries 3 and 16).

We carried out additional experiments that allowed us to obtain useful information about the very high activity and stability of catalyst A. First, the IR spectrum of the catalyst was recorded (Bruker Tensor 27). The bands at 1614 and 1419, 1456, and 2945 cm⁻¹ can be attributed to the C=N and CH₃ groups in the TMG cation, thus indicating that this cation is present in the catalyst.

The X-ray photoelectron spectrum of the as-prepared catalyst A was collected on an ESCALab220i-XL spectrometer operating at 15 kV and 20 mA at a pressure of about 3 × 10⁻⁹ mbar with Al K_α radiation as the excitation source (*hν* = 1486.6 eV). In the survey XPS analysis for catalyst A no Cl could be detected, which suggests that RuCl₃ is completely

[*] S. Miao, Dr. Z. Liu, Prof. B. Han, Dr. J. Huang, Z. Sun, Dr. J. Zhang, Dr. T. Jiang
Center for Molecular Science
Institute of Chemistry
Chinese Academy of Sciences
Beijing 100080 (P.R. China)
Fax: (+86) 10-6256-2821
E-mail: liuzm@iccas.ac.cn

[**] This work was financially supported by the National Natural Science Foundation of China (20374057, 50472096) and the Opening Research Fund of the State Key Laboratory of Heavy Oil Processing (2004-10).

Table 1: Hydrogenation of benzene with different catalysts.

Entry	Catalyst	Benzene/Ru [mol/mol]	T [°C]	P(H ₂) [MPa]	t [h]	Yield [%] ^[a]	TOF ^[b]
1	A	1000	40	2.0	2.5	84.5	–
2	A	1000	40	4.0	2.5	100	400
3	A	1000	40	6.0	1.8	100	555
4	A	1000	40	8.0	1.5	100	667
5	A	10000	110	8.0	2.5	100	4000
6 ^[c]	A	10000	110	8.0	2.5	100	4000
7 ^[c]	A	10000	110	8.0	2.5	100	4000
8 ^[c]	A	10000	110	8.0	2.5	100	4000
9 ^[c]	A	10000	110	8.0	2.5	100	4000
10	B	1000	40	4.0	2.5	100	400
11	B	10000	110	8.0	2.5	100	4000
12	C	1000	40	4.0	2.5	54.0	–
13	C	1000	40	6.0	2.5	94.2	376
14	D	1000	40	4.0	2.5	44.5	–
15	Ru/C ^[d]	1000	40	4.0	5.0	99.5	200
16	Ru/C ^[d]	1000	40	6.0	2.5	98.5	394
17	Ru/Al ₂ O ₃ ^[e]	1000	40	4.0	3.5	35.6	102
18	Ru/Al ₂ O ₃ ^[e]	1000	60	4.0	4.5	79.5	177

[a] Yield of cyclohexane. [b] TOF (turnover frequency) was calculated as conversion of mols of benzene per mol of Ru per hour. [c] Catalyst A was reused for a further four runs. [d] Ru/C, 5% Ru on carbon powder, from ICI Co., Japan. [e] Ru/Al₂O₃, 5% Ru on Al₂O₃ powder, provided by XiAA Catal. Chem. Tech. Co. Ltd., China.

converted into the metal under the conditions used. Figure 1 shows the Ru 3d spectrum of the composite. It can be seen that although the Ru 3d signal is obscured by the C 1s signal of

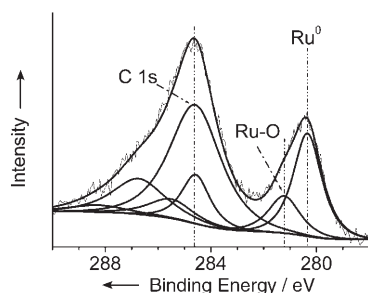


Figure 1. XPS spectra at the Ru 3d edge of catalyst A. The three vertical lines indicate the peak positions of the binding energies of C 1s, Ru–O, and Ru, respectively.

a carbon contaminant at 284.6 eV, the deconvoluted spectrum shows a doublet for two chemically different Ru entities with peak binding energies of 280.3 (Ru 3d_{5/2}) and 284.5 eV (Ru 3d_{3/2}), which confirms the presence of Ru⁰ in catalyst A.^[14] Moreover, the peak at 281.1 eV suggests the presence of a Ru–O component, which probably results from oxidation of the ruthenium nanoparticles upon exposure to air.

Similar phenomena have also been reported by other groups.^[10c,d] The XPS results indicate that the RuCl₃ loaded on MMT is reduced to Ru⁰ by hydrogen at 220 °C within 2 h. This reaction temperature is lower than those commonly used.^[10e] The reduction in the reaction temperature probably results from the interaction of RuCl₃ with the IL and/or the substrate. A similar phenomenon has also been reported by Zhuang and co-workers, who reduced RuCl₃ and H₂PtCl₆ dispersed on activated carbon with hydrogen at 120 °C.^[15]

The N₂ sorption isotherms of pristine MMT, TMG-exchanged MMT, and catalyst A were determined with an ASAP-2405N instrument at liquid-nitrogen temperature after degassing the samples at 200 °C and 10^{−4} Torr for 12 h. They show type-IV characteristics, thereby indicating the mesoporous structures of these samples. According to the nitrogen-desorption data, the specific surface area increases from 37 m²g^{−1} for pristine MMT to 43 m²g^{−1} for TMG-exchanged MMT and 57 cm²g^{−1} for catalyst A due to the loading of Ru nanoparticles.

We also characterized the catalysts by means of X-ray diffraction (XRD) with an X'PERT SW diffractometer (40 kV, 40 mA, Cu_{Kα} radiation) in the small-angle range of 2θ = 1–12° and the wide-angle range of 2θ = 4–70°.

On the basis of the XRD analysis in the small-angle range (Figure 2), the basal spacing of pristine MMT is 0.966 nm, while the spacing of TMG-exchanged MMT is enlarged to d₀₀₁ = 1.42 nm due to

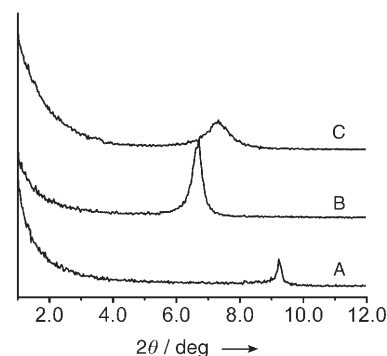


Figure 2. XRD patterns of A) pristine MMT, B) TMG-exchanged MMT, C) TMG-MMT/Ru (catalyst A).

the incorporation of the organic cations of the IL into the galleries of MMT upon ion exchange. The characteristic peak of catalyst A is shifted slightly to wider angle relative to the peak of TMG-MMT, which suggests the intercalation of Ru nanoparticles in the interlayers of MMT. However, there is no diffraction peak for Ru nanoparticles in the XRD pattern in the wide-angle range (not shown), which implies that the Ru particles are either very small or amorphous.

The morphology of catalyst A was investigated with a transmission electron microscope (TEM, JEOL, JEM-2010) equipped with an energy-dispersive X-ray spectrometer (EDS) at an accelerating voltage of 200 kV. It can be seen that irregular nanoparticles with a size of less than 3 nm are uniformly distributed on the MMT surfaces (Figure 3a). These were confirmed as Ru particles by EDS analysis during

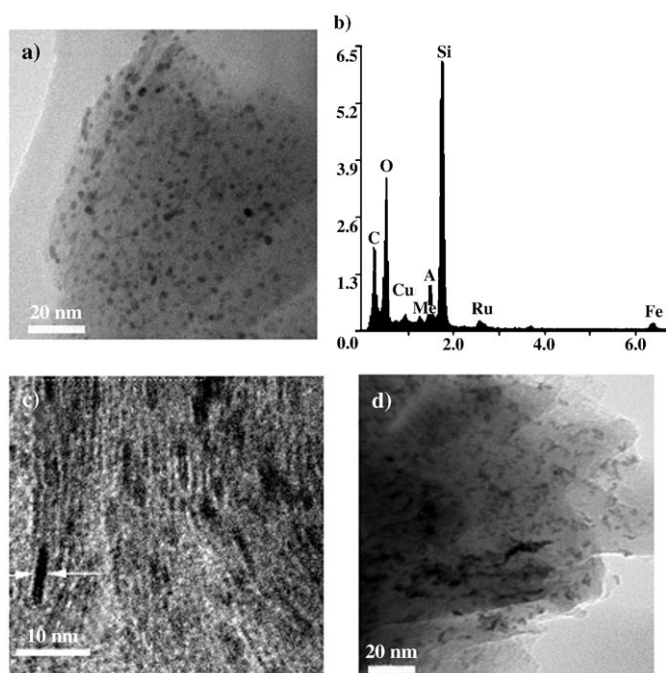


Figure 3. a) TEM image of fresh catalyst A, b) EDS analysis of catalyst A, c) HRTEM image of a cross-section of catalyst A. The white arrows indicate the interlamellar space of montmorillonite intercalated with an Ru nanoparticle, d) TEM image of catalyst A after five runs.

the TEM observation (Figure 3b). No large particles were found on MMT. The nanoparticles are firmly immobilized on MMT and could not be removed from the substrate even when the catalyst was treated ultrasonically for a long time.

To detect whether Ru nanoparticles are present in the interlayers of MMT, we embedded catalyst A in epoxy resin to form a solid specimen, and cut the specimen with an ultramicrotome to get an ultrathin section of the catalyst, which was examined by high-resolution TEM (HRTEM). Figure 3c shows an HRTEM image of the section of catalyst A. The layered structure of MMT in catalyst A can be clearly seen from this image, and the interlamellar spacing is about 1.2 nm (as indicated by the white arrows in Figure 3c), which is consistent with the XRD results. Moreover, there are many nanoparticles of less than 1.2 nm in the interlamellar spaces of MMT, thus indicating that Ru nanoparticles are intercalated into the MMT interlayers. This means that the Ru nanoparticles exist in the catalyst in two forms: some are present on the outer surfaces and others are embedded in the interlayers. We believe that both these kinds of Ru nanoparticles catalyze the hydrogenation of benzene. We also obtained the morphology of catalyst A after five catalytic cycles by TEM (Figure 3d). It can be seen that the nanoparticles on the MMT surface tend to aggregate. However, as discussed above, the activity of catalyst A does not decrease significantly after five runs. This may imply that the Ru particles in the interlayers play the main role in the high activity of the catalyst, and that most of the Ru particles are in the interlayers.

Using a similar procedure to that used to prepare catalyst A, we prepared catalyst B by thoroughly washing

the TMG-MMT/RuCl₃ composite with water to remove the soluble Ru³⁺ before hydrogen reduction. In other words, the only difference in the procedures for preparing catalyst A and catalyst B is that the water-soluble Ru³⁺, which could be precipitated and mixed with the MMT/Ru composite during the vaporization process, is removed before hydrogen reduction when preparing catalyst B, while all of the Ru³⁺ is reduced when preparing catalyst A. Catalyst B displays a similar catalytic activity for benzene hydrogenation to catalyst A, which suggests that the Ru³⁺ in the RuCl₃ aqueous solution is firmly fixed onto the TMG-exchanged MMT during the soaking process.

We also treated pristine MMT directly with the aqueous solution of RuCl₃ in the absence of the IL (catalyst C), and we synthesized catalyst D by treating MMT with 1-*n*-butyl-3-methylimidazolium tetrafluoroborate ([bmim][BF₄]), another IL, in a similar manner to catalyst A. Both catalysts C and D exhibit much lower activity for the hydrogenation of benzene than catalysts A and B, as shown in Table 1. Therefore, it can be deduced that the TMG cations present in catalysts A and B play an important role in immobilizing the Ru nanoparticles on MMT.

It has been reported that guanidine and guanidinium readily form coordination complexes.^[16] On the basis of results reported in the literature and our experimental results we can propose a possible mechanism for the formation of catalyst A. During the treatment of MMT with the aqueous solution of [TMG][TFA] the cations of the IL exchange with the Na⁺ ions present in the interlayers of pristine MMT to form the TMG-exchanged MMT, which has a larger interlayer spacing than MMT, as confirmed by XRD analysis. In the subsequent process to load Ru³⁺ onto the TMG-exchanged MMT, some Ru³⁺ ions could diffuse into the enlarged MMT interlayers, whilst others are distributed on the outer surface, due to the coordination between TMG and Ru³⁺. This coordination between TMG and Ru³⁺ is favorable to the loading of Ru³⁺. Finally, Ru⁰ nanoparticles are produced by reduction of Ru³⁺ with H₂. Thus, for catalyst A, the TMG cations interact strongly with the surface of MMT by electrostatic forces and at the same time they stabilize Ru nanoparticles by coordination due to their electron-donor ability.^[16]

In this way, Ru⁰ nanoparticles could be prepared on an MMT support by a combination of electrostatic forces and coordination. Both the electrostatic and coordination forces are very strong, which results in a very stable catalyst. The Ru⁰ nanoparticles in the interlayers of MMT are very small, which may be a reason for the very high activity for benzene hydrogenation. The TEM study clearly showed that some Ru nanoparticles are distributed on the outer MMT surfaces, and that these could not be separated from the MMT even after lengthy ultrasonic treatment. Therefore, the nanoparticles on the outer surface may also be stabilized by the IL.

In summary, we presented a method to prepare Ru nanocatalysts using [TMG][TFA] and MMT. In this method the IL is first exchanged with the ions in the clay, and then Ru³⁺ ions are loaded onto the IL-exchanged MMT. The final Ru/MMT nanocatalyst is obtained after hydrogen treatment. This catalyst shows very high activity for the hydrogenation of

benzene and is very stable, due to the excellent synergistic effects of TMG, MMT, and Ru nanoparticles. We believe that other transition metals, such as Rh, Pd, and Ir, could also be supported on MMT using this method and the resulting materials could be used as efficient nanocatalysts.

Experimental Section

Preparation of the catalyst: Na montmorillite with a cation-exchange capacity (CEC) of 1.0 meq g^{-1} was supplied by Hongyan Mining Co. We only describe the preparation of catalyst A because the procedures to prepare catalysts B, C, and D are nearly the same and have been described briefly above. In the experiment to synthesize catalyst A, about 1.0 g of MMT was dispersed in an aqueous solution of the IL by stirring for about 4 h. The molar ratio of IL to the CEC of MMT was 1.1:1. The MMT was then separated from the solution by centrifugation and was treated again with an aqueous solution of the IL. This procedure was repeated three times. The IL-exchanged MMT was then washed several times with distilled water. The exchanged MMT was dispersed in 5 mL of an aqueous solution of RuCl_3 with a concentration of 8 mg mL^{-1} . The water was then removed by evaporation. The final Ru/MMT catalyst was obtained after hydrogenation of the solid at 220°C for 2 h. The mass content of Ru in the composite was 3.3 wt. %, which was calculated based on the amounts of clay and RuCl_3 added.

Hydrogenation of benzene: The reactions were carried out in a 20-mL, stainless-steel autoclave equipped with a magnetic stirrer. In a typical experiment, 87 mg of Ru nanocatalyst and 2.0 g of benzene were placed in the autoclave and the air was replaced by H_2 within 10 min. The reaction mixture was stirred (300 rpm) at the desired temperature. More hydrogen was added to reach the pressure of interest. After the appropriate time the temperature was lowered to room temperature quickly in an ice-water bath and the hydrogen pressure was released. The products were analyzed by GC (Agilent 4890 D).

Received: July 27, 2005

Revised: October 10, 2005

Published online: November 28, 2005

Keywords: clays · heterogeneous catalysis · hydrogenation · ionic liquids · ruthenium

- [1] a) J. Dale, M. Kowalska, D. L. Cocke, *Chemosphere* **1991**, *22*, 769; b) J. Sterte, *Clays Clay Miner.* **1986**, *34*, 658.
- [2] a) T. J. Pinnavaia, *Science* **1983**, *220*, 365; b) A. Gil, L. M. Gandia, M. A. Vicente, *Catal. Rev. Sci. Eng.* **2000**, *42*, 145; c) "Pillared Clays": R. Burch in *Catalysis Today*, Vol. 2, Elsevier, New York, **1988**, p. 185; d) J. L. Valverde, A. de Lucas, P. Sánchez, F. Dorado, A. Romero, *Appl. Catal. B* **2003**, *43*, 43; e) B. M. Choudary, M. L. Kantam, K. V. S. Ranganath, K. K. Rao, *Angew. Chem.* **2005**, *117*, 326; *Angew. Chem. Int. Ed.* **2005**, *44*, 322; f) B. Veisz, Z. Király, L. Tóth, B. Pécz, *Chem. Mater.* **2002**, *14*, 2882; g) M. D. Nikalje, A. Sudalai, *Tetrahedron* **1999**, *55*, 5903; h) D. Dolmazov, R. Aldea, H. Alper, *J. Mol. Catal. A: Chem.* **1998**, *136*, 147; i) L. X. Shao, M. Shi, *Adv. Synth. Catal.* **2003**, *345*, 963; j) J. S. Yadav, B. V. S. Reddy, A. K. Raju, D. Gnaneshwar, *Adv. Synth. Catal.* **2002**, *344*, 938; k) Z. H. Han, H. Y. Zhu, S. R. Bulcock, S. P. Ringer, *J. Phys. Chem. B* **2005**, *109*, 2673.
- [3] Z. Király, B. Veisz, Á. Mastalir, Gy. Köfaragó, *Langmuir* **2001**, *17*, 5381–5387.
- [4] T. Kawabata, T. Mizugaki, K. Ebitani, K. Kaneda, *J. Am. Chem. Soc.* **2003**, *125*, 10486.
- [5] S. Papp, J. Szél, A. Oszkó, I. Dékány, *Chem. Mater.* **2004**, *16*, 1674.
- [6] a) T. Welton, *Chem. Rev.* **1999**, *99*, 2071; b) P. Wasserscheid, W. Keim, *Angew. Chem.* **2000**, *112*, 3926; *Angew. Chem. Int. Ed.* **2000**, *39*, 3772; c) M. J. Earle, K. R. Seddon, *Pure Appl. Chem.* **2000**, *72*, 1391; d) "Ionic Liquids as Green Solvents: Progress and Prospects", *ACS Symp. Ser.* **2003**, 856.
- [7] L. A. Blanchard, D. Hancu, E. J. Beckman, J. F. Brennecke, *Nature* **1999**, *399*, 28.
- [8] a) J. Dupont, G. S. Fonseca, A. P. Umpierre, P. F. P. Fichtner, S. R. Teixeira, *J. Am. Chem. Soc.* **2002**, *124*, 4228; b) Y. Zhou, M. Antonietti, *J. Am. Chem. Soc.* **2003**, *125*, 14960; c) K. S. Kim, D. Demberelynamba, H. Lee, *Langmuir* **2004**, *20*, 556.
- [9] J. Huang, T. Jiang, H. Gao, B. Han, Z. Liu, W. Wu, Y. Chang, G. Zhao, *Angew. Chem.* **2004**, *116*, 1421; *Angew. Chem. Int. Ed.* **2004**, *43*, 1397.
- [10] a) T. Naota, H. Takaya, S.-I. Murahashi, *Chem. Rev.* **1998**, *98*, 2599; b) O. Vidoni, K. Philippot, C. Amiens, B. Chaudret, O. Balmes, J. O. Malm, J. O. Bovin, F. Senocq, M. J. Casanova, *Angew. Chem.* **1999**, *111*, 3950; *Angew. Chem. Int. Ed.* **1999**, *38*, 3736; c) K. Pelzer, O. Vidoni, K. Philippot, B. Chaudret, V. Colliere, *Adv. Funct. Mater.* **2003**, *13*, 118; d) E. T. Silveira, A. P. Umpierre, L. M. Rossi, G. Machado, J. Morais, G. V. Soares, I. J. R. Baumvol, S. R. Teixeira, P. F. P. Fichtner, J. Dupont, *Chem. Eur. J.* **2004**, *10*, 3734; e) V. A. Mazzieri, P. C. L'Argentièrre, F. Coloma-Pascual, N. S. Figoli, *Ind. Eng. Chem. Res.* **2003**, *42*, 2269; f) C. M. Hagen, L. Vieille-Petit, G. Laurenczy, G. Süß-Finke, R. G. Finke, *Organometallics* **2005**, *24*, 1819; g) L. M. Rossia, G. Machadao, P. F. P. Fichtnerb, S. R. Teixeirac, J. Duponta, *Catal. Lett.* **2004**, *92*, 149; h) G. S. Fonseca, E. T. Silveira, M. A. Gelesky, J. Dupont, *Adv. Synth. Catal.* **2005**, *347*, 847.
- [11] H. X. Gao, B. X. Han, J. C. Li, T. Jiang, Z. M. Liu, W. Z. Wu, Y. H. Chang, J. M. Zhang, *Synth. Commun.* **2004**, *34*, 3083.
- [12] G. Süß-Finke, M. Faure, T. R. Ward, *Angew. Chem.* **2002**, *114*, 105; *Angew. Chem. Int. Ed.* **2002**, *41*, 99.
- [13] P. J. Dyson, D. J. Ellis, D. G. Parker, T. Welton, *Chem. Commun.* **1999**, 25.
- [14] J. F. Moulder, W. F. Stickle, P. E. Sobol, K. D. Bomben in *Handbook of X-ray Photoelectron Spectroscopy*, Perkin-Elmer, Eden Prairie, MN, **1992**.
- [15] B. Yang, Q. Y. Lu, Y. Wang, L. Zhuang, J. T. Lu, P. F. Liu, *Chem. Mater.* **2003**, *15*, 3552.
- [16] a) S. Aoki, K. Iwaida, N. Hanamoto, M. Shiro, E. Kimura, *J. Am. Chem. Soc.* **2002**, *124*, 5256; b) P. J. Bailey, S. Pace, *Coord. Chem. Rev.* **2001**, *214*, 91.